IEEE Access
Multidisciplinary | Rapid Review | Open Access Journal

Received November 13, 2018, accepted December 13, 2018, date of publication December 25, 2018,
date of current version January 16, 2019.

Digital Object Identifier 10.1109/ACCESS.2018.2889684

Indoor Collaborative Positioning With Adaptive Particle-Pair Filtering Based on Dynamic User Pairing

XIAOFENG LU[1], KUN YANG[2], (Senior Member, IEEE), JIAYU LIU[1], CHANGLIN YANG[1], ZIBO ZHANG[1], AND HAILIN ZHANG[1]

[1]State Key Laboratory of Integrated Services Networks, Xidian University, Xi'an 710126, China
[2]School of Computer Science and Electronic Engineering, University of Essex, Colchester CO4 3SQ, U.K.

Corresponding author: Xiaofeng Lu (luxf@xidian.edu.cn)

This work was supported in part by the Key Research and Development Plan of Shaanxi Province under Grant 2018ZDCXL-GY-04-06, and in part by the National Natural Science Foundation of China under Grant 61371127, Grant 61572389, Grant 61620106011, Grant 61671347, and Grant U1705263.

ABSTRACT Technologies fusing WiFi-based indoor positioning and pedestrian dead reckoning for indoor target localization have already been proposed for a variety of occasions. Among them, the methods of multisource fusion with particle filter perform well in a random noise environment. However, the positioning accuracy can be significantly affected by the personnel density of the interest area. In this paper, we propose a novel indoor collaborative positioning system which performs dynamic user pairing and adaptive particle-pair filtering with the help of the Chirp acoustic signal distance measurement. The proposed scheme mainly includes two parts in each time slot: first, the users are clustered into cells for dynamic user-pairing, and then the adaptive particle-pair filter iterates the comprehensive weight to obtain the final positioning result. The experiment results show that the proposed scheme can effectively solve the problem of the error increase caused by the intensive personnel, and remarkably improve the indoor positioning accuracy in the crowded public.

INDEX TERMS Indoor positioning, dynamic user pairing, acoustic distance measurement, adaptive particle-pair filter.

I. INTRODUCTION

In recent years, with the continuous increase in the number of giant buildings and underground malls, location based service (LBS) in indoor condition has been receiving wide attention among the society and academia. At present, the existing indoor localization technologies are mainly based on iBeacon, WiFi, Radio Frequency Identification (RFID), visible light communications (VLC), ZigBee and Ultra Wide-band (UWB) [1]–[5]. Detailed comparisons can be referred in [1].

With the rapid advancement of intelligent terminals, the existence of wireless Local Area Network (WLAN) has become the infrastructure of large-scale buildings. Indoor positioning technology based on WLAN is one of the hotspots due to its relatively low cost and wide coverage [6], [7], [8], and WiFi-based indoor positioning method is typically complemented with other technologies such as PDR, Kalman filter, or particle filter, etc. References [9]–[11] proposed schemes that fusing WiFi location and other positioning technologies by extended Kalman filter. Reference [12] provided a study on the improvement of particle filter for indoor positioning. The particle filter also can be applied in various scenarios, such as in [13] that mobile target tracking with particle filter can be realized underwater by autonomous vehicle. Reference [14] introduced a map matching technology using variations in the ambient magnetic field for indoor navigation. Reference [15] implemented particle filter in road crack identification. Seeing the fusion capability of the particle filter, we chose it to perform the collaborative filtering in our system. To obtain a robust positioning performance, [16] introduced a system fusing UWB sensor-based positioning solution with inertial measurement unit (IMU) via an Extended Kalman Filter (EKF).

On some occasions reported in previous studies [17], [18], however, the accuracy can not satisfy requirements of high accuracy because of the low stability of the WiFi positioning.

Especially under the personnel intensive condition, the block of random moving dense personnel can cause loss, reflection and other interference on the propagation of WiFi signal, leading to extreme instability in accurate localization.

In this paper, we propose a novel system that transforms the disadvantage of the dense personnel into the key to eliminate the decrease of accuracy caused by the crowd, where the particle-pair filter is introduced here to achieve the purpose. First, positioning participants (users for short) are selected and combined into user-pairs as many as possible with inexistence of co-channel interference guaranteed. Then the multisource information including PDR data, WiFi coarse positioning result and the real-time distance measurement are added into the improved system based on the conventional particle filter algorithm. Under the condition of personnel intensive, the system enhances the correction effect on inaccurate WiFi positioning results and obtains more accurate positioning results.

The rest of this paper is organized as follows: In section 2, the system is constructed and the main infrastructures applied in the system are introduced. Section 3 explains the dynamic user pairing (DUP) algorithm and the adaptive particle-pair filter respectively. In section 4, the experiments are built to demonstrate the performance of the proposed system and comparison are made between the proposed approach and several related methods. Section 5 depicts the implementation and testing of the system. Finally, section 6 concludes the paper.

II. SYSTEM OVERVIEW

In this section, first the system architecture of the proposed scheme is stated. Then the infrastructures applied in the system are respectively described in part B including: WiFi positioning module, trajectory forecasting module and distance measurement module.

A. SYSTEM ARCHITECTURE

We implemented our proposed scheme in a system architecture that includes a server, N WiFi access hot spots $\{AP_1...AP_N\}$ and U independent users noted as $m \in \{1, 2..., U\}$ moving randomly in an indoor interest region with an area of S. Each user is equipped with a intelligent terminal utilized to complete two tasks: 1.collecting the received signal strength indication (RSSI) and the IMU data, 2.transmitting & receiving the Chirp signals for distance measurement. The IMU data measured by the inertial measurement unit (IMU) embedded in intelligent terminals, the RSS data and the acoustic distance measurement are uploaded into the server via APs which act as relays between the server and the users. The server acts as the central processor completing the data reception, the DUP, the adaptive particle-pair filtering and the results provision.

Depicted in Fig.1, the DUP algorithm can be described as the following process: At time slot T_1, suppose that the user A, B, and C are in the same cell, userB and userC are selected as a user-pair and the distance $S_{T_1}^{BC}$ between them are

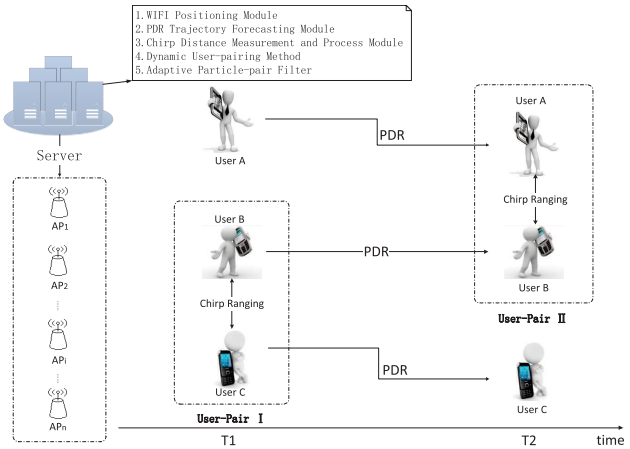

FIGURE 1. The scene model of the indoor collaborative positioning system.

measured by Chirp ranging. Their precise positioning results are collaboratively obtained by adaptive particle-pair filter, while the other users in the cell, like userA, are positioning independently at this time slot. Then at time slot T_2, the previous partnership will be dissolved and another user-pair such as userA and userB is selected based on the real-time distance between them. Processing by the adaptive particle-pair filter, the outputs of the server are sent to terminals for display.

B. INFRASTRUCTURES APPLIED IN THE SYSTEM

1) WiFi POSITIONING MODULE

In the server, coarse positioning is completed by the RSSI fingerprint based localization method pioneered by Jian and Hao [19]. The process of coarse positioning includes two phases [20]; the first phase is the offline stage whose main task is to establish a WiFi fingerprinting database that contains the RSSI on each reference spot collecting from the WiFi access points (APs) existing nearby; the second phase is the online phase. In this phase, coarse positioning results will be acquired through the k-Nearest Neighbor (kNN) algorithm. At time slot k, the WiFi positioning result of the user m is noted as ${Y_k}^{(m)}(m = 1...U)$.

2) TRAJECTORY FORECASTING MODULE

Trajectory forecasting is achieved by PDR [21], [22]. Since current intelligent mobile terminals are usually equipped with the inertial measurement unit (IMU), i.e. accelerometer, gyroscope, PDR can be employed to infer the real-time trajectory of human by the help of the IMU.

PDR automates the position prediction based on the previous known position, the distance traveled and direction of travel. PDR position calculation formula can be expressed as follows.

$$\begin{pmatrix} x_{k+1} \\ y_{k+1} \end{pmatrix} = \begin{pmatrix} x_k \\ y_k \end{pmatrix} + \begin{pmatrix} \Delta l \times \cos\varphi \\ \Delta l \times \sin\varphi \end{pmatrix} \quad (1)$$

where $\begin{pmatrix} x_k \\ y_k \end{pmatrix}$ is the coordinates of last location and Δl is the step length and φ is the angle of walking direction.

However, PDR can only offer the relative displacement and rotation direction from the last state, as (1) shows. In order to get the absolute trajectory of user, the intelligent terminal is required to indicate a start or end point in floor plan. In addition, the main disadvantage of PDR is the accumulation of drift error along with time, which makes the single PDR algorithm not suitable for accurate indoor localization.

3) DISTANCE MEASUREMENT AND PROCESS MODULE

Once the server selects two adjacent users as a user-pair, the distance measurement module is triggered to measure the distance between the two users [23]. The Chirp signal is utilized here to accomplish distance measurement owing to its good frequency band utilization, strong anti-interference and high accuracy which has been proven in [24]–[26]. The theoretical ranging error of Chirp acoustic distance measurement is only $d_e = v/F_s \approx 0.07m$, so we consider the ranging result S_k equivalent to the actual distance. The process of the Chirp acoustic distance measurement between deviceA and deviceB is shown in Fig. 2.

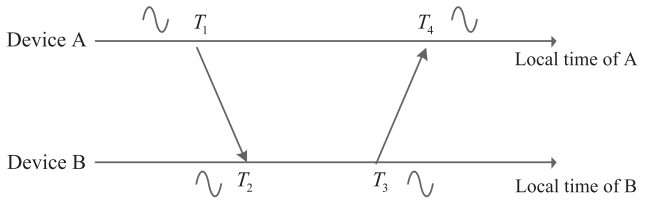

FIGURE 2. The principle of Chirp acoustic distance measurement.

The time that the acoustic wave spreads between two terminals are measured and used to calculate the distance.

$$S_k^{AB} = v * \frac{(T_4 - T_1) - (T_3 - T_2)}{2} \tag{2}$$

where S_k^{AB} stands for the distance between deviceA and deviceB, T_1 and T_4 are the local time of deviceA, and T_2 and T_3 are the local time of deviceB, and v is the speed of acoustic wave spreading in the air which is around 340m/s.

III. ADAPTIVE PARTICLE-PAIR FILTERING BASED ON DUP

The whole system consists of five modules with unique algorithms including three pre-existing algorithms and two novel algorithms that we proposed. In the following paragraphs, the novel algorithms will be expatiated respectively.

The algorithms are implemented in their belonging modules on the server side.These Algorithms include:

1) WiFi positioning based on RSSI fingerprint database,
2) Dynamic user pairing,
3) Chirp acoustic distance measurement,
4) trajectory forecasting based on PDR method,
5) adaptive particle-pair filtering.

As depicted in Fig.3, first, based on the IMU measurement data, the trajectory prediction of the user is generated through the PDR algorithm and the coarse position is obtained by the WiFi positioning scheme. Then user-pairs are selected and allocated with distinguished channels of Chirp signal through the DUP algorithm. Finally the distance measurement is sent to the adaptive particle-pair filter along with the coarse position and the predicted position, and the final positioning results will be generated here.

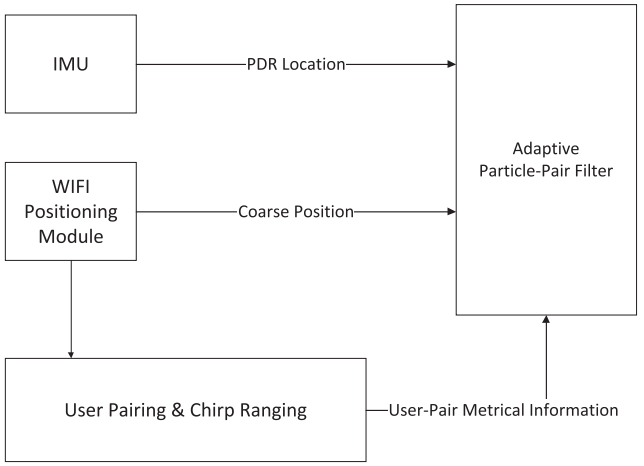

FIGURE 3. The interior architecture of the indoor collaborative positioning system.

A. DUP ALGORITHM

In each time slot, the algorithm can be boiled down into the following two parts: user pairing and channel allocation for cells. The FDMA of Chirp signal and the concept of user-pair distance are introduced as follows:

1) FDMA OF CHIRP SIGNAL

The advantages of using Chirp signal for distance measurement include high multipath resolution, strong noise immunity and low transmitting power. Besides, Chirp signal also has the superiorities of low cost, long transmission distance, small volume and high speed for daily use.

The high-frequency section of the audible frequencies is usually chosen for acoustic ranging, in which 6.5-18.5 kHz is audible to human ears [27] while less noticeable. In order to enable multiple user-pairs to perform acoustic ranging meanwhile in a personnel intensive area, this algorithm takes advantage of the bandwidth of Chirp signal in the frequency domain, and segments the complete band into 5 subbands, with 0.5kHz between each subband as a protection interval. Therefore, 5 kinds of Chirp signal that can be distinguished by handheld intelligent terminals are obtained. To avoid serious error caused by co-channel interference, these 5 signals are allocated to different user-pairs in the region in each timeslot. The specific channel segmentation is shown in Table 1.

2) DEFINITION AND CALCULATION OF USER-PAIR DISTANCE

Enlightened by the advanced solution to resource allocation using cellular networks [28], we propose the DUP algorithm to realize cell clustering and optimal channel allocation of

TABLE 1. Channel segmentation.

Subband	Bandwidth
I	6.5kHz - 8.5kHz
II	9kHz - 11kHz
III	11.5kHz - 13.5kHz
IV	14kHz - 16kHz
V	16.5kHz - 18.5kHz

Chirp signals according to the user-pair distances. Therefore, we first define the rule of user-pair distance.

For two user-pairs P^M and P^N; P^M is represented as $P^M = \{p_a, p_b\}$, where p_a and p_b represent the two users; and P^N is represented as $P^N = \{p_c, p_d\}$, where p_c and p_d represent the two users. The Euclidean distance d_{mn} $(m, n \in \{p_a, p_b, p_c, p_d\}, m \neq n)$ between any two users among p_a, p_b, p_c, p_d is

$$d_{mn} = \left| {Y_k}^{(m)} - {Y_k}^{(n)} \right| \quad (m, n \in \{p_a, p_b, p_c, p_d\}, m \neq n) \tag{3}$$

Therefore, the user-pair distance of P^M and P^N can be defined as

$$D^{MN} = \min\{d_{mn}\} \quad (m, n \in \{p_a, p_b, p_c, p_d\}, m \neq n) \tag{4}$$

Since the system uses adaptive particle-pair filtering as a significant method to improve the positioning accuracy, the nearest two users are preferred to combine as a user-pair in DUP. Many public indoor areas have the characteristic of dense and uneven distribution of personnel, thus in order to quickly select user-pairs as many as possible to perform filtering collaboratively, Affinity Propagation (AP) [29], algorithm is chosen to implement the initial clustering. Compared with the classical clustering algorithms including K-means algorithm, K-centers algorithm, CLARANS algorithm and so on, AP algorithm has the following advantages:

1) AP algorithm does not need to establish the number of final clustering families;
2) Compared with the classical K-means algorithm, the existing data points are used as the final clustering center instead of creating a new cluster center which may not exist. It is suitable for the following pairing methods: select the closest user to the cluster head and complete the pairing;
3) The AP algorithm model is insensitive to the initial value of the data;
4) The AP algorithm has no requirement for the symmetry of the initial similarity matrix data;
5) Compared with the K-centers clustering method, the squared error of the result is smaller. So this paper uses AP clustering algorithm.

The AP algorithm can be expressed by the following formulas and the Euclidean distance is chosen to evaluate the similarity in the AP algorithm.

1) Similarity matrix S:

$$s(m, n) = -||Y_k^{(m)} - Y_k^{(n)}||^2, \quad \forall m, n \in \{1, 2, ..., U\}, m \neq n \tag{5}$$

2) Calculation of the initial preference p_1:

$$p_1 = \gamma \cdot median\{s(m, n), \quad \forall m, n \in \{1, 2, ..., U\}, m \neq n\} \tag{6}$$

where γ is a coefficient that needs to be adjusted according to the actual situation and its value determines the number of clusters. The optimal preference p^{opt} will be obtained by iteration based on the correlation between the preference p_i and the number of user-pairs.

3) Responsibility Matrix R :

$$r(m, n) = s(m, n) - \max_{n' \neq n} \{a(m, n') + s(m, n')\}, \quad m \neq n \tag{7}$$

$$r(n, n) = s(n, n) - \max_{n' \neq n} \{a(n, n') + s(n, n')\}, \quad m = n \tag{8}$$

4) Availability Matrix A :

$$a(m, n) = \min\left\{0, r(n, n)^{(o)} + \sum_{m' \neq m, n} \max\{0, r(m', n)^{(o)}\}, \quad m \neq n \right. \tag{9}$$

$$a(n, n)^{(o)} = \sum_{m' \neq n} \max\{0, r(m', n)\}, \quad m = n \tag{10}$$

Cluster centers generated through iterations are $O_k^v (v = 1...V)$, where V represents the number of clusters based on the preference p_i.

It is obvious that the number of clusters is negatively related to the number of users in each cluster. Therefore, we can control the result of clustering by iterating the preference p_i. Based on the principle of Voronoi diagram, the mid-normals of the lines connecting adjacent cluster centers are interconnected as shown in Fig.4(a), so the interest area can be divided into V successive cells and each cell contains a complete cluster, as depicted in Fig.4(b). In the later process, we consider a cell as the minimum unit of user set to complete the Chirp channel allocation and the performance optimization.

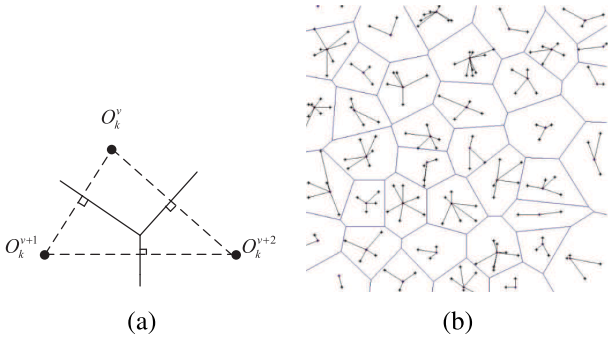

FIGURE 4. (a) Cell division strategy based on the Voronoi diagram. (b) Correlation between cells and clusters.

Two users who have the shortest distance between them are paired in each cell for the accuracy of acoustic distance measurement. The adaptive particle-pair filter must be implemented on users in the same cluster, besides the positioning accuracy will be significantly improved with the increase of filtering times according to the theory of particle filter. So we select two users whose possibility to leave the corresponding cluster in a time slot are lowest, that is, the user-pair is constructed by each cluster center with its closest user. We assumed that the cluster M contains I users, and the cluster center O_k^M is stationary. In this cluster, we select the user ϵ ($\epsilon \in 1...I$) who has the shortest distance $d_{\epsilon M}$ from O_k^M, and combine ϵ with O_k^M to build a user-pair P^M which performs the Chirp acoustic distance measurement and the collaborative filtering in the current time slot. The distance D^{MN} between user-pairs P^M and P^N is calculated according to (3) and (4), and D^{MN} is used to determine whether the co-channel interference exists between them. According to the chromatic number algorithm proposed by [30], the channel allocation method based on user-pair distance is proposed.

When the distance D^{MN} between user-pairs P^M and P^N is shorter than the co-channel distance l, the relationship between P^M and P^N is marked as connected; otherwise, disconnected. All user-pairs form a vertex set and all user connection relations form a connection set, so a connected graph $G = (V, E)$ is constructed, where V represents the vertex set and E represents the connection set. Referred to the chromatic number algorithm, the vertex set V is divided into j same-color-blocks noted as $S_1, S_2, ..., S_j$ which can be colored respectively by colors $1^{\#}, 2^{\#}, ..., j^{\#}$. That is, the vertex chromatic number $x(G) = j$. $x(G)$ represents the minimum of Chirp channels that enable all user-pairs in the region to perform distance measurement simultaneously. The criteria for calculating the optimal preference is:

1) The initial p_1 is the average of the similarity matrix $s(m, n)$;
2) $x(G)$ is obtained through the chromatic number algorithm;
3) It is known from the DUP algorithm that the number of user-pairs has a positive correlation with the number of Chirp channels required to guarantee no co-channel interference in the region. Based on the correlation between the number of chirp signals and the preference $|p_i|$, the optimal preference p^{opt} is iterated through the following formula:

$$|p_{i+1}| = \alpha \left[x(G) - x(G)_{\max}\right] + |p_i| \quad i=1...n \tag{11}$$

where i represents the number of iterations; it is known from the last paragraph that the initial preference p_1 is the average of $s(m, n)$, and the number of Chirp channels $x(G)_{\max} = 5$. The coefficient of iteration $\alpha \approx 0.1$. The algorithm terminates when $x(G) = x(G)_{\max}$, and $p_i = p_{i+1}$ which derives the optimal preference $p^{opt} = p_i$. Finally, p^{opt} is used for clustering. After clustering, those 5 Chirp signals are utilized for the channel allocation according to the chromatic number algorithm.

B. ADAPTIVE PARTICLE-PAIR FILTER

Based on Bayesian theory, particle filter was first introduced in [31] as an attempt to solve estimation tasks in the context of state-space modeling for more general nonlinear and non-Gaussian scenarios. Because precise positioning results can not be obtained by any of the following methods alone, we proposed adaptive particle-pair filter to fuse PDR data, WiFi coarse positioning result and the real-time distance measurement by conducting joint filtering for a pair of users simultaneously.

1) BAYESIAN THEORY APPLIED TO MOTION TRACKING

In Bayesian filter method, the motion model of a user can be established as the following form:

$$x_k = f_k(x_{k-1}, \eta_k) \tag{12}$$
$$y_k = h_k(x_k, v_k) \tag{13}$$

where $f_k(\cdot)$ and $h_k(\cdot)$ are nonlinear functions. The random vector x_k is the state vector and y_k corresponds to the observations. The dimensions of x_k and y_k can be different. η_k and v_k represent two independent noise sequences: state noise and process noise.

In Bayesian theory point of view, the solution to the state estimation is to recursively calculate the credibility of the current state based on the previous series of existing data $y_{1:k}$. The credibility is the probability density $p(x_k\,|y_{1:k})$, which requires recursive calculations by two stages: forecast stage and update stage.By the nature of Bayesian network and the assumption of the first-order Markov process of the model,in advance we can write

$$p(y_k\,|x_k,\ y_{1:k-1}) = p(y_k\,|x_k) \tag{14}$$

and

$$p(x_k\,|x_{k-1},\ y_{1:k-1}) = p(x_k\,|x_{k-1}) \tag{15}$$

- Stage 1: forecast stage $p(x_k\,|y_{1:k-1})$ can be obtained from the probability density of the last time slot $p(x_{k-1}\,|y_{1:k-1})$:

$$\begin{aligned} p(x_k\,|y_{1:k-1}) &= \int p(x_k, x_{k-1}\,|y_{1:k-1})dx_{k-1} \\ &= \int p(x_k\,|x_{k-1},\ y_{1:k-1})p(x_{k-1}\,|y_{1:k-1})dx_{k-1} \\ &= \int p(x_k\,|x_{k-1})p(x_{k-1}\,|y_{1:k-1})dx_{k-1} \end{aligned} \tag{16}$$

- Stage 2: update stage During this stage, the posterior probability $p(x_k\,|y_{1:k})$ will be obtained through the following equations by $p(x_k\,|y_{1:k-1})$ which indicates the forecast of the state x_k. With the measurement value in the time slot k added, $p(x_k\,|y_{1:k})$ serves as the modification of the forecast, and later it will be substituted into

the next forecast stage to form another recursion.

$$p(x_k\,|y_{1:k}) = \frac{p(y_k\,|x_k,\ y_{1:k-1})p(x_k\,|y_{1:k-1})}{p(y_k\,|y_{1:k-1})} = \frac{p(y_k\,|x_k)p(x_k\,|y_{1:k-1})}{p(y_k\,|y_{1:k-1})} \tag{17}$$

where the normalization constant is

$$p(y_k\,|y_{1:k-1}) = \int p(y_k\,|x_k)p(x_k\,|y_{1:k-1})dx_k = Z_k \tag{18}$$

We have used (14) in the deduction of (17) because according to the measurement equation, the vector y_k is only related to the vector x_k.

Indeed, the previous recursions can be compactly expressed as

$$p(x_k\,|y_{1:k}) = \underbrace{\frac{p(y_k\,|x_k)}{Z_k}}_{corrector}\underbrace{\int p(x_k\,|x_{k-1})p(x_{k-1}\,|y_{1:k-1})dx_{k-1}}_{predictor} \tag{19}$$

2) THE PRINCIPLE OF ADAPTIVE PARTICLE-PAIR FILTERING

We hypothesized that two users p_a and p_b walk independently in the location region and they are selected as a user-pair $P^M = \{p_a, p_b\}$ at the time slot k. Their motion models are as follows:

$$\begin{cases} X_k = f_k(X_{k-1}, \eta_k) \\ Y_k = h_k(X_k, v_k) \end{cases} \quad motion\ model\ of\ p_a \tag{20}$$

$$\begin{cases} X'_k = g_k(X'_{k-1}, \eta_k) \\ Y'_k = z_k(X'_k, v_k) \end{cases} \quad motion\ model\ of\ p_b \tag{21}$$

where $f_k(\cdot)$, $h_k(\cdot)$, $g_k(\cdot)$, and $z_k(\cdot)$ are nonlinear functions. The random vector X_k and X'_k are the state vectors corresponding to the forecasted positions of p_a and p_b; Y_k and Y'_k stand for the observations i.e. the WiFi positioning results. The dimensions of X_k and Y_k can be different. Since the motion model of p_a and p_b are of the same form, the following description of X_k also applies to X'_k, similarly to Y_k and Y'_k. η_k and v_k respectively represent state noise and process noise which are two independent noise sequences.

For user p_a of the user-pair $P^M = \{p_a, p_b\}$, $f(X_k)$ is the function to indicate the position coordinates of the state X_k, and $p(X_k\,|Y_{1:k})$ is the posterior probability density which represents the credibility of the state X_k. Let $X_k^{(i)}$ $i \in (1:N)$ denote the state of the particle i, $W_k^{(i)}$ its weight, and N the number of particles. The positioning result of p_a can be expressed as

$$E\,[f(X_k)] = \int f(X_k)p(X_k\,|Y_{1:k})dX_k = \int f(X_k)\frac{p(X_k\,|Y_{1:k})}{q(X_k\,|Y_{1:k})}q(X_k\,|Y_{1:k})dX_k = \int f(X_k)w_k(X_k)q(X_k\,|Y_{1:k})dX_k \tag{22}$$

among the above equations

$$w(X_k) = \frac{p(X_k\,|Y_{1:k})}{q(X_k\,|Y_{1:k})} \tag{23}$$

Initially, the particles are equal-weighted samples from the initial prior $q(x_0)$. At each time instant, the weight is recursively calculated by the following procedure:

$$q(X_{1:k}\,|Y_{1:k}) = q(X_{1:k-1}\,|Y_{1:k-1})q(X_k\,|X_{1:k-1}, Y_{1:k}) \tag{24}$$

The recursive form of the posterior probability density function can be expressed as

$$p(X_{1:k}\,|Y_{1:k}) = \frac{p(Y_k\,|X_{1:k}, Y_{1:k-1})p(X_{1:k}\,|Y_{1:k-1})}{p(Y_k\,|Y_{1:k-1})} = \frac{p(Y_k\,|X_k)p(X_k\,|X_{k-1})p(X_{1:k-1}\,|Y_{1:k-1})}{p(Y_k\,|Y_{1:k-1})} \tag{25}$$

The recursive form of the weight of the particle can be expressed as

$$w_k^{(i)} = w_{k-1}^{(i)}\frac{p(Y_k\,|X_k^{(i)})p(X_k^{(i)}\,|X_{k-1}^{(i)})}{q(X_k^{(i)}\,|X_{1:k-1}^{(i)}, Y_{1:k})} = w_{k-1}^{(i)}p(Y_k\,|X_k^{(i)}) \tag{26}$$

where the proposal distribution

$$q(X_k\,|X_{1:k-1}, Y_{1:k}) = q(X_k\,|X_{1:k-1}, Y_k) = p(X_k\,|X_{1:k-1}) \tag{27}$$

The integral calculation of (22) can be solved by the Monte Carlo method, so that

$$E\,[f(X_k)] \simeq \frac{1}{N}\sum_{i=1}^{N} w(X_k^{(i)})f(X_k^{(i)}) = \frac{\sum_{i=1}^{N} w(X_k^{(i)})f(X_k^{(i)})}{\sum_{i=1}^{N} w(X_k^{(i)})} \tag{28}$$

The single-user weight of p_a, $w(X_k^{(i)})$ can be obtained by recursion as (26):

$$w_k^{(i)} = w_{k-1}^{(i)}p(Y_k\,|X_k^{(i)}) = \frac{1}{N}\prod_{n=2}^{k} p(Y_n\,|X_n^{(i)}) \tag{29}$$

Equally, the corresponding notations X'_k, $X'^{(j)}_k$, $W'^{(j)}_k$, and N are declared for user p_b and the single-user weight of user p_b can be obtained.

For the user-pair consisting of p_a and p_b, the initial particle distributions of them are set as independent Gaussian distributions with different variances and means, which are

$$X_1^{(i)} \sim N(\mu_1, \sigma_1) \qquad X'^{(j)}_1 \sim N(\mu'_1, \sigma'_1) \tag{30}$$

We assign the current WiFi positioning results Y_k and Y'_k of p_a and p_b to μ_k, μ'_k respectively. According to (30),

we can get the particle distributions of p_a and p_b at the time slot k as

$$\begin{aligned} X_k^{(i)} &\sim N(\mu_k, \sigma_k) \\ X'^{(j)}_k &\sim N(\mu'_k, \sigma'_k) \end{aligned} \tag{31}$$

where

$$\begin{aligned} \mu_k &= X_k + \zeta_k \\ \mu'_k &= X'_k + \delta_k \end{aligned}$$

and ζ_k denotes the error vector between the PDR forecasted position of p_a and its WiFi positioning result, similarly to δ_k of p_b.

Each particle of p_a can form a particle pair with each particle of p_b, that is, a total of N^2 particle pairs will be generated in a model of two existing users. Due to the independence between p_a and p_b, the probability density of the distance between the particle i of p_a and the particle j of p_b can be expressed as

$$p(d_k^{(ij)}) = p(\left|X_k^{(i)} - X'^{(j)}_k\right|) \tag{32}$$

Then, according to "the difference between two independent Gaussian distributions still obeys Gaussian distribution", so the distribution of $d_k^{(ij)}$ can be obtained:

$$\begin{aligned} d_k^{(ij)} &= \left|X_k^{(i)} - X'^{(j)}_k\right| \\ &\sim N(\left|\mu_k - \mu'_k\right|, \sigma_k + \sigma'_k)\ (d_k^{(ij)} \geq 0) \end{aligned} \tag{33}$$

As shown in the Fig.5, at the time slot k, the distance between users p_a and p_b is noted as S_k^{ab} which is measured by the Chirp acoustic ranging technology; i, j, and $j+1$ represent different particles of p_a and p_b; $d_k^{(ij)}$ stands for the distance between particle i and j. According to the principle of distance measurement with Chirp acoustic signal, the maximum value of S_k^{ab} is the maximum distance that the acoustic signal can reach (about 10m). Focusing on the particle of p_a, let i combines with every particle j ($j = 1...N$) of p_b so a set of N particle-pairs, which is noted as $\chi_k^{(i)}$, will be obtained, and the weight of $\chi_k^{(i)}$ is $\varphi_k^{(i)}$. Note that the posterior probability density of $\chi_k^{(i)}$ equals the mean posterior probability density of each $d_k^{(ij)}$ ($j = 1...N$) based on the distance S_k^{ab} and the coarse position of p_a that is Y_k. The particle-pair weight $\varphi_k^{(i)}$ can be expressed as

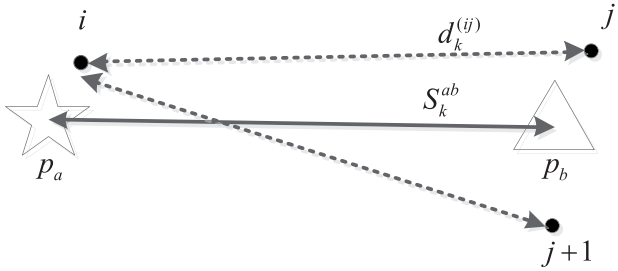

FIGURE 5. The schematic diagram of the particle pairing.

$$\begin{aligned} \varphi_k^{(i)} &= p(\chi_k^{(i)} \left| S_{1:k}^{ab}, Y_{1:k} \right.) \\ &= \frac{1}{N}\sum_{j=1}^{N} p(d_k^{(ij)} \left| S_k^{ab}, Y_k \right.) \\ &= \frac{1}{N}\sum_{j=1}^{N} p(\left|X_k^{(i)} - X'^{(j)}_k\right| \left| S_k^{ab}, Y_k \right.) \\ &= p(\frac{\sum_{j=1}^{N}\left|X_k^{(i)} - X'^{(j)}_k\right|}{N} \left| S_k^{ab}, Y_k \right.) \\ &= \varphi_{k-1}^{(i)} \cdot p(S_k^{ab} \left| \chi_k^{(i)}, Y_k \right.) \end{aligned} \tag{34}$$

We define $p(S_k^{ab} \left| \chi_k^{(i)}, Y_k \right.)$ as

$$p(S_k^{ab} \left| \chi_k^{(i)}, Y_k \right.) = \frac{1}{\sqrt{2\pi}\sigma} \exp\left[-\frac{1}{2\sigma^2}\cdot(\frac{1}{N}\sum_{j=1}^{N} d_k^{(ij)} - \mu)^2\right] \tag{35}$$

where

$$\mu = S_k$$

Furthermore, the sharper the distribution of p_a, the greater the distinction among the particle pair cloud. That is, the variance of (35) affects the degree of discrimination of particle-pair weights. In order to make the novel PF effects better, we tend to adopt the following strategies: decreasing σ to increase the confidence of particles with high similarity and to reduce the confidence of particles with low similarity. After repeated experiments, we choose $\sigma = 0.05$.Then the particle-pair weight $\varphi_k^{(i)}$ is iterated by

$$\begin{aligned} \varphi_k^{(i)} &= \varphi_{k-1}^{(i)} p(S_k \left| \chi_k^{(i)}, Y_k \right.) \\ &= \varphi_{k-1}^{(i)} \cdot \frac{1}{\sqrt{2\pi}\sigma} \exp\left[-\frac{1}{2\sigma^2}\cdot(\frac{1}{N}\sum_{j=1}^{N} d_k^{(ij)} - S_k)^2\right] \end{aligned} \tag{36}$$

When a user p_c moves distantly from the user community, the clustering procedure may assign it alone into a cell, which causes p_c unable to combine with other users as user-pairs. Aimed at this case, p_c is considered as a user-pair P_k^{cc} itself. For the user-pair P_k^{cc}, $d_k^{(ii)}$ is considered to be a constant value close to infinitesimal on any particle i_m of p_c. That is

$$S_k^{cc} = 0 \approx d_k^{(i)} \tag{37}$$

Therefore, $\varphi_k^{(i_m)}$ is a constant value at a specific time slot k

$$\begin{aligned} \varphi_k^{(i)} &= \varphi_{k-1}^{(i)} \cdot \frac{1}{\sqrt{2\pi}\sigma} \exp(-\frac{(d_k^{(ii)} - S_k^{cc})^2}{2\sigma^2}) \\ &= \varphi_1^{(i)} \left(\frac{1}{\sqrt{2\pi}\sigma}\right)^{k-1} \\ &= \frac{1}{N\left[\sqrt{2\pi}\sigma\right]^{k-1}} \end{aligned} \tag{38}$$

According to the collaborative filtering pattern we proposed, the comprehensive weight $\upsilon_k^{(i)}$ of particle i is the product of the single-user weight $w_k^{(i)}$ and the user-pair weight $\varphi_k^{(i)}$ as

$$\upsilon_k^{(i)} = w_k^{(i)} \cdot \varphi_k^{(i)} \tag{39}$$

known by(26)and(36),

$$\begin{aligned} w_k^{(i)} &= w_{k-1}^{(i)} p(Y_k \left| X_k^{(i)} \right.) \\ \varphi_k^{(i)} &= \varphi_{k-1}^{(i)} p(S_k \left| \chi_k^{(i)}, Y_k \right.) \end{aligned} \tag{40}$$

So the comprehensive weight is expressed as

$$\begin{aligned} \upsilon_k^{(i)} &= w_k^{(i)} \cdot \varphi_k^{(i)} \\ &= w_{k-1}^{(i)} p(Y_k \left| X_k^{(i)} \right.) \cdot \varphi_{k-1}^{(i)} p(S_k \left| \chi_k^{(i)}, Y_k \right.) \\ &= \upsilon_{k-1}^{(i)} \cdot \frac{p(X_k^{(i)}, Y_k)}{p(X_k^{(i)})} \cdot \frac{p(X_k^{(i)}, X'_k, Y_k, S_k)}{p(X_k^{(i)}, X'_k, Y_k)} \\ &= \upsilon_{k-1}^{(i)} \cdot \frac{p(X_k^{(i)}, X'_k, Y_k, S_k)}{p(X_k^{(i)}) p(X'_k)} \\ &= \upsilon_{k-1}^{(i)} p(S_k, Y_k \left| \chi_k^{(i)} \right.) \end{aligned} \tag{41}$$

Then $\upsilon_k^{(i)}$ is normalized as

$$\vartheta_k^{(i)} = \frac{\upsilon_k^{(i)}}{\sum_{i=1}^{N} \upsilon_k^{(i)}} \tag{42}$$

The final filtering result output by the adaptive particle-pair filter is

$$E\left[f(X_k)\right] = \sum_{i=1}^{N} \vartheta(X_k^{(i)}) f(X_k^{(i)}) \tag{43}$$

For the user-pair p_k^{cc},

$$\begin{aligned} \upsilon_k^{(i)} &= w_k^{(i)} \cdot \varphi_k^{(i)} \\ &= \frac{w_k^{(i)}}{N\left[\sqrt{2\pi}\sigma\right]^{k-1}} \end{aligned} \tag{44}$$

After normalization,

$$\vartheta_k^{(i)} = \frac{\upsilon_k^{((i)}}{\sum_{i=1}^{N} \upsilon_k^{(i)}} = \frac{w_k^{(i)}}{\sum_{i=1}^{N} w_k^{(i)}} = W(X_k^{(i)}) \tag{45}$$

The filtering result of p_a, that is, the final positioning result will be

$$E\left[f(X_k)\right] = \sum_{i=1}^{N} W(X_k^{(i)}) f(X_k^{(i)}) \tag{46}$$

where $W(X_k^{(i)})$ is the normalized weight of $w_k^{(i)}$.

Then the resampling is performed on particle set $\left\{i, \upsilon_k^{(i)}\right\}$ once a positioning process is completed, and the new particle set $\left\{i', 1/N\right\}$ is obtained for the next positioning process.

IV. IMPLEMENTATION AND EVALUATION

A. SYSTEM IMPLEMENTATION

We design the indoor collaborative positioning system based on the proposed algorithm. In this system, RSSI of mobile terminals are transmitted to the server, Media Access Control (MAC) Address of them are collected by AP groups, and acceleration and deflection information of users are detected by the IMU of their intelligent terminals. Chirp acoustic distance measurement is realized between two terminals that belong to the same user-pair, and fingerprint matching of the coarse positioning, dynamic user pairing and particle-pair filter are all realized in the server. The indoor collaborative positioning system is mainly composed of three parts, as shown in Fig.6.

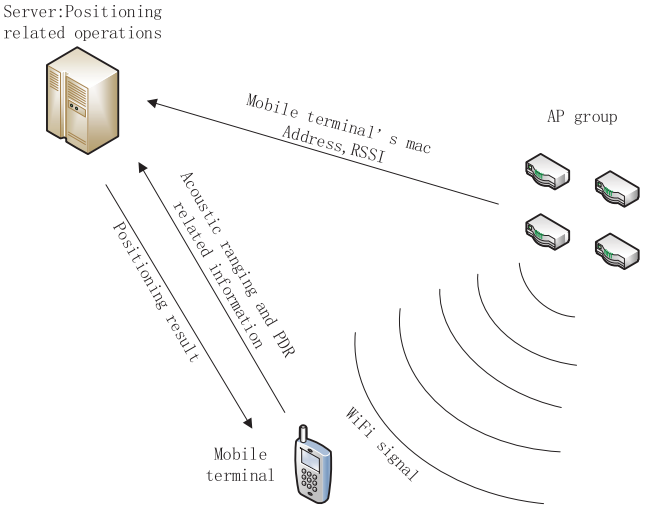

FIGURE 6. Systematic architecture diagram of the indoor collaborative positioning system.

1) Mobile terminal: As the client-side, mobile terminals usually carry Android or iOS system which have IMU for PDR including acceleration sensors and geomagnetic sensors. During the positioning process, the terminals need to complete the following tasks: continuously collecting the information from the sensor and transmitting it to the server in real time; booting the WiFi positioning module to enable the AP group to obtain the RSSI of the terminals; receiving the positioning coordinates from the server feedback and displaying them on the terminals; and when the collaborative positioning process is turned on, the terminals perform the distance measurement between users according to instructions from the server.
2) Access Point (AP) group: AP represents the router that connects multiple users' terminals. The mobile terminal receives the electromagnetic wave transmitted by the AP group and detects the RSSI matrix as the location fingerprint information for the WiFi coarse positioning. In this paper, the routing development board MT7620A which is equipped with OpenWrt system is utilized to analyse the performance of the WiFi coarse positioning, and it is called a intelligent AP. The main

work of the AP group in the positioning system is to transmit information.

3) Server: At the server-side, the information obtained by AP group and intelligent terminals are used to carry out calculation, and the adaptive particle-pair filter and the dynamic user pairing method are completed. If a intelligent terminal is not connected to the WiFi network, the data transmission can still be completed through the mobile network.

As shown in Fig.7, before the positioning operation, the client-side has been realized in the Android system of intelligent terminals, the server-side has been realized in the Windows system on computer and AP group is already set on. After the server obtains the WiFi positioning coordinates of the users, users are clustered according to the dynamic user-pairing algorithm. After the user-pairs are formed, the two users in each user-pair are coordinated by the server for Chirp acoustic ranging. The server obtains acoustic ranging results and PDR information of all users, then runs particle-pair filtering algorithm proposed in this paper. Finally, the cooperative location results are sent to each client-side, and the final location results are displayed on the map stored in advance on the client-side. TCP protocol is used for transmit information between the client-side and the server-side.

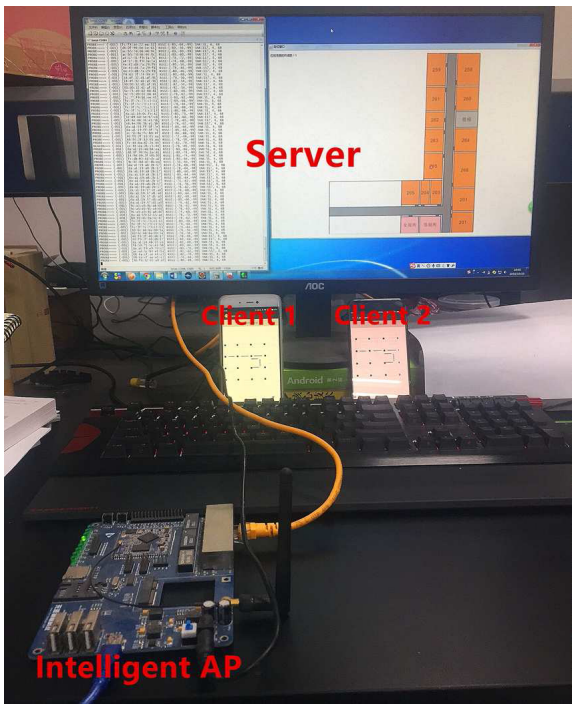

FIGURE 7. Two mobile terminals simulate two users, MT7620A is used as an AP and the computer is the server.

B. EVALUATION METHODOLOGY

The experiments are conducted in the certain indoor region of $50 \times 50m^2$in the main building of Xidian University. Fig.8 is the map of the experiment region with the distribution of the intelligent Access Points (AP) and the reference points (RP) shown in. The uniformly distributed red points represent different reference points, and 52 APs are located in the edges of the region. In advance, an Android smartphone is placed in each RP in sequence to collect RSSI of the AP group and a fingerprint database is established and saved in the server-side. It is known that many objects are placed in the laboratories and the corridors outside the laboratories are filled with passerby who walk frequently, which conforms to the complex indoor environment of the proposed algorithm.

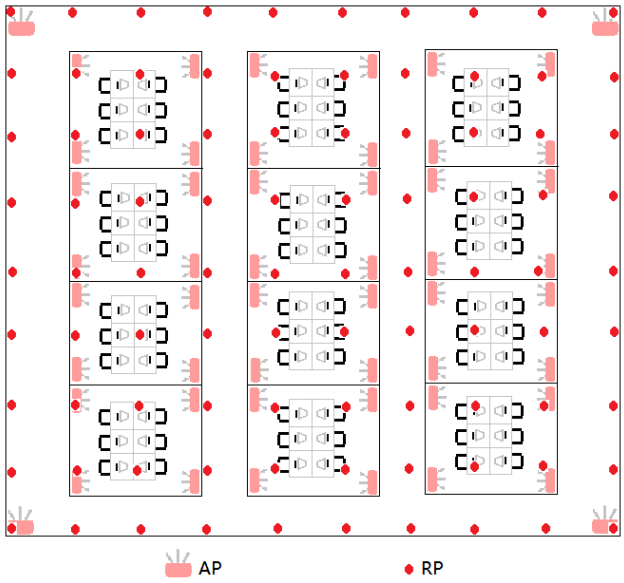

FIGURE 8. Distribution of AP and reference points in laboratory.

200 experiment participants each carries an Android smartphone are walking randomly at the speed of 1 m/s in the experiment region. Fig.9 shows the distribution of the experiment participants at a moment.

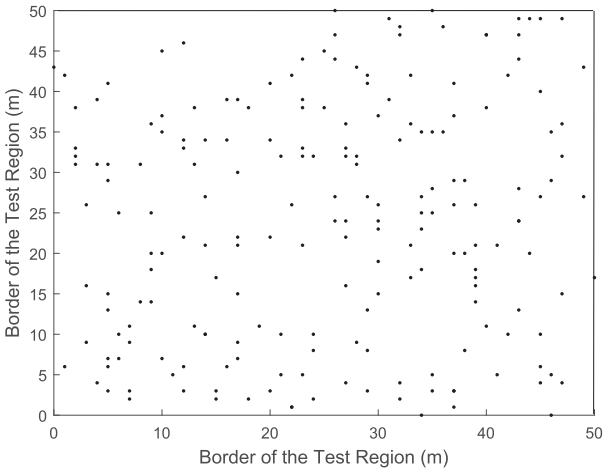

FIGURE 9. 200 users random distribution diagram.

In the process of experiments, a target user performs uniform motion along a specific test route shown in Fig.10 while other users are moving randomly. The motion model of the

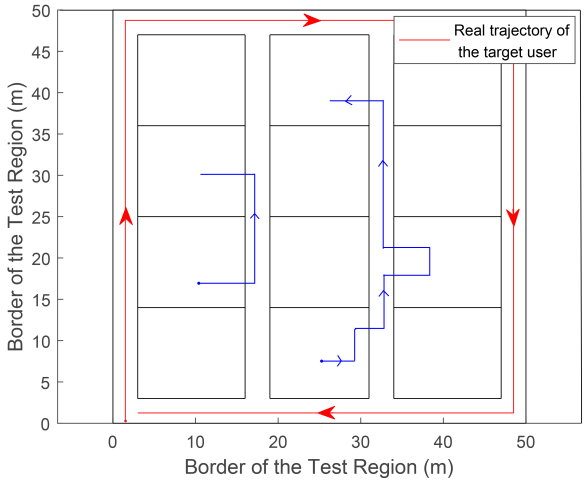

FIGURE 10. The test route of the target user.

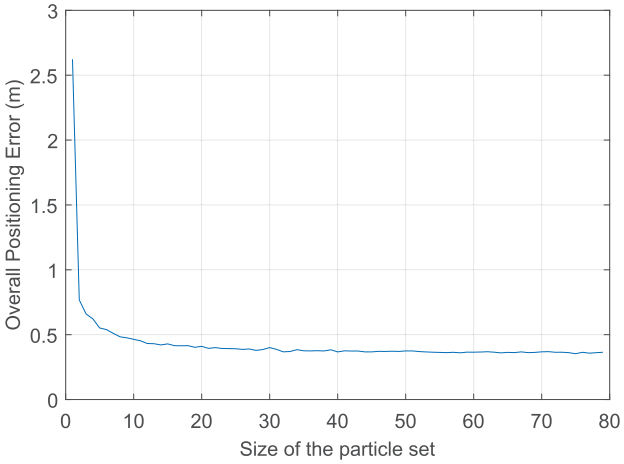

FIGURE 11. The overall positioning error of the proposed scheme vs. the number of particles applied in the adaptive particle-pair filter.

target users is

$$X_k \,|X_{k-1} \sim N(X_{k-1} + \Delta l, \varepsilon)$$

where Δl is the footstep length of the average person, and ε means the state noise of PDR equation. The details of the experiment parameters are shown in Table 2.

TABLE 2. Experiment parameters.

Parameter	Value
N	40
ε	0.04m
Δl	50cm

In order to comprehensively analyze the performance of the indoor collaborative positioning system, two types of positioning error are presented. When a user requests to obtain his current location information at a certain location in the experimental area, the system automatically calculates the location of the user for 24 times and output the average value of these positioning results obtained from the 24 times as the user's final positioning results. Therefore, the definition of the "average positioning error" is: the average of the distance difference between the 24 positioning results and the actual position. "overall positioning error" is noted as the evaluation of the overall performance of a positioning algorithm. The definition of the overall positioning error is the average of the positioning errors of the users involved in the experiment. Fig.11 shows that the average positioning error decreases with the increase of the size of the particle set applied in the filter in general, which coincides with the Monte Carlo theory. However, as the number of particles increases, it has less influence on the performance of the system, besides particle redundancy will make the localization process complicated and time-consuming. Here we consider the relationship between the average positioning error and the number of particles, thus select the size of the particle set to be 40.

C. EXPERIMENTAL RESULTS AND COMPARISON WITH RELATED TECHNOLOGIES

Fig.12(a)-(c) depict the process of dynamic user-pairing in a time slot. As shown in Fig.12(a), the participants are divided into several clusters through the clustering approach. Then the user-pairs each consisted of a cluster center represented by red star and its nearest user represented by black star is generated as Fig.12(b). As shown in Fig.12(c), the cells are allocated with 5 colors standing for different channels.

Fig.13 depicts the trace tracks of the target user when using different positioning methods. Obviously, the performance of PDR is the worst since its positioning accuracy decreases rapidly over time, whereas the track of the target user group using the proposed scheme is remarkably close to the real trajectory shown in Fig.10.

The CDF diagrams of average positioning errors of six different technologies are generated, so the comparison of the average positioning error between different technologies can be obtained from Fig.14. It can be observed that more than 78% average positioning error is less than 0.5m. Besides, compared with the traditional KNN+ PDR+ particle filter positioning scheme, the probability of the average positioning error less than 0.5m is increased by 24%, and the probability of error less than 0.8m is increased by 13%.

The performances which are evaluated by the overall positioning error of the proposed system and some related methods can be sketched as Table 3.

Fig.15 shows the fluctuations of performance of our proposed system and the single user particle filter based positioning scheme at different density of personnel existing in the interest area. From the figure we can see that under the low density of personnel environment, the overall positioning errors of these two schemes are roughly similar. With the increase of the personnel density from 0.04 person per square

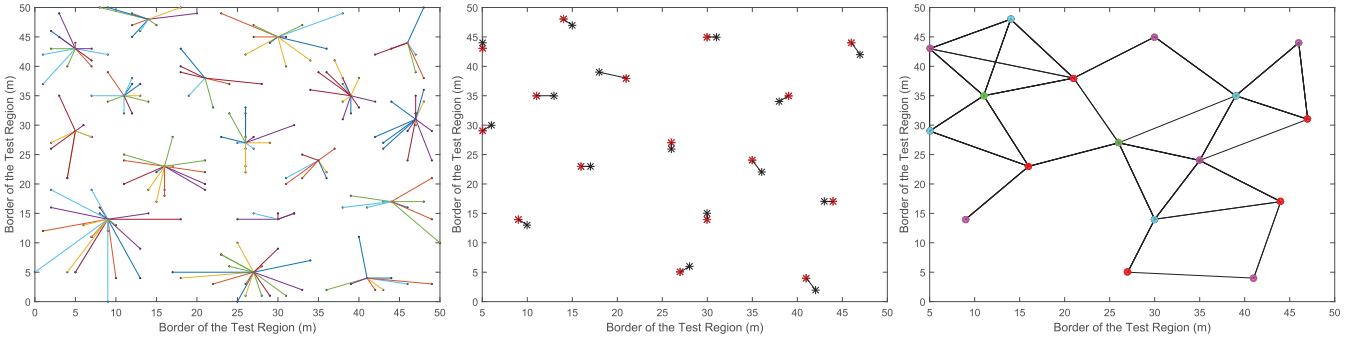

FIGURE 12. (a) The clusters of users. (b) The selected user-pairs. (c) The channel allocation of cells.

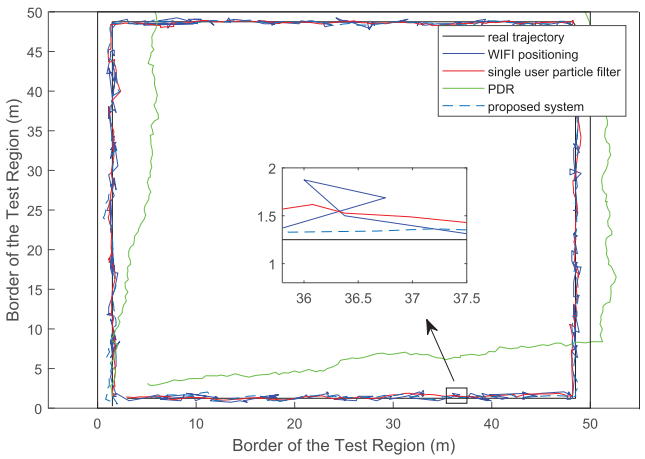

FIGURE 13. Positioning trace of the target user by five different method.

TABLE 3. Overall positioning error of a few technologies.

Method	Overall error(m)
PDR	3.64
WIFI	0.96
Single-user PF	0.52
Proposed scheme	0.36

meter to 0.4 person per square meter, the overall positioning error of the proposed scheme increases 0.57m, whereas the other increases 1.77m. Therefore, it can be concluded that the robustness of the proposed method against dense personnel interference has a very superior performance.

It can be seen from the analysis of several experimental results that the positioning accuracy of the system is also affected by the accuracy of the PDR prediction, as shown in Fig.16. Obviously, because that the overall positioning error increases with the variance of PDR equation, the accuracy has a negative correlation with the variance of PDR equation which determines the error of PDR. And it can be observed from Fig.16 that the proposed scheme is less affected by the error of PDR than the single user particle filter, which means our indoor positioning system has a strong adaptability on different qualities of intelligent terminals.

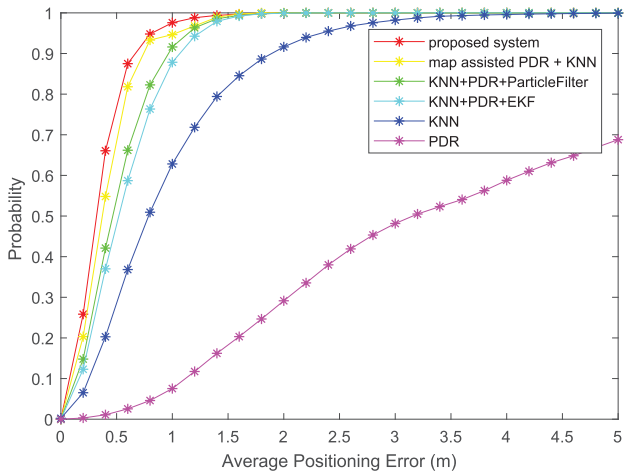

FIGURE 14. Comparison of average positioning error among different schemes.

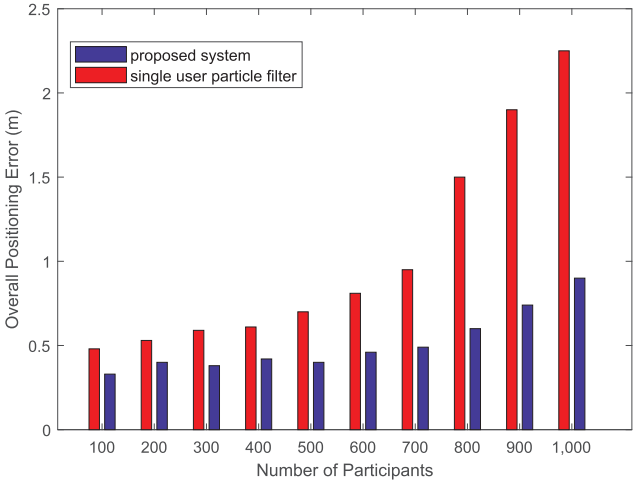

FIGURE 15. Overall positioning error at different density of personnel.

D. THE ANALYSIS OF THE PERFORMANCE OF INDOOR COLLABORATIVE POSITIONING SYSTEM

In order to evaluate the performance of the indoor collaborative positioning algorithm, the time consumption of all the processes in the positioning system are separately

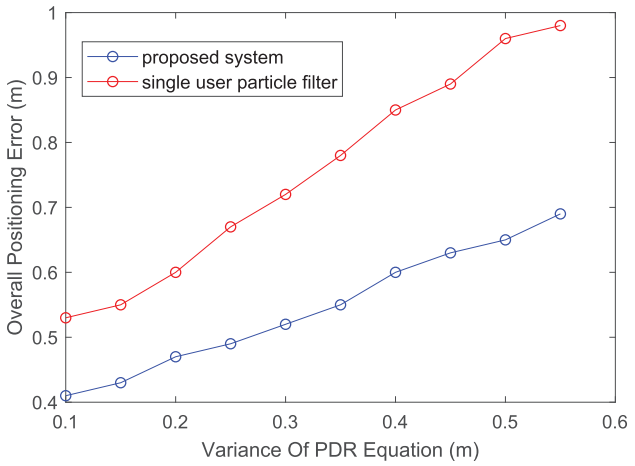

FIGURE 16. Overall positioning error vs. the error of PDR.

measured during the experiments, including the WiFi positioning method, the dynamic user pairing algorithm, the Chirp acoustic ranging process and the particle-pair filter. During the experiments, the number of reference points is 64 and the number of users is 100. The measurement results are shown in Table 4. As can be seen from Table 4, the time consumption of each process of the positioning system is extremely short, which fully satisfies the real-time performance of the positioning system.

TABLE 4. Time consumption of processes in the positioning system.

Process	Experiment(ms)
WIFI positioning method	8
Dynamic user pairing algorithm	14
Chirp acoustic ranging process	70
Particle-pair filter	1
Total consumption	93

Different performance of the positioning accuracy caused by different walking speed of the users are also measured during the experiments. When the walking speed of the users are 1 m/s, 2 m/s, 3 m/s and 4 m/s, the real-time positioning error are shown in Table 5. According to the data, the walking speed of normal adults is 2 m/s. In the actual environment, the users' walking speed are set to 1 to 4 m/s. It can be seen from Table 5 that, although the positioning error of the system increases with the user's walking speed, the average positioning error of the positioning system is only 0.530 m when the user's walking speed is 4 m/s. To sum up, the positioning performance of the proposed algorithm is better than most positioning technologies, so the system can be called an accurate indoor positioning system.

TABLE 5. Real-time positioning performance.

Speed(m/s)	1	2	3	4
Overall Positioning error(m)	0.390	0.413	0.470	0.530

V. CONCLUSIONS

In this paper, we have proposed a novel and efficient scheme which constructs user-pairing dynamically and fuses the WiFi-based indoor positioning, PDR and Chirp acoustic signal distance measurement with the adaptive particle-pair filter. Aiming at the obstacle that the density of personnel seriously affects the accuracy of WiFi positioning, the algorithm specializes in fusing the multisource information to obtain more accurate location information in a collaborative pattern of positioning in a random noise environment.

Repeated experiments on a actual scenario demonstrate that, our proposed approach addressed the decrease of positioning accuracy caused by the intensive personnel in the interest area. The overall error of the proposed positioning system is 0.36 m, which is nearly 3 and 2 times smaller than that of WiFi-based positioning and single user particle filter positioning system respectively. In summary, the overall accuracy of the proposed system can meet the requirement for high precision localization and tracking under the condition of personnel intensive.

REFERENCES

[1] N. Ul Hassan, A. Naeem, M. A. Pasha, T. Jadoon, and C. Yuen, "Indoor positioning using visible LED lights: A survey," *ACM Comput. Surv.*, vol. 48, pp. 1–32, 2015, Art. no. 20.
[2] C. Yang and H.-R. Shao, "WiFi-based indoor positioning," *IEEE Commun. Mag.*, vol. 53, no. 3, pp. 150–157, Mar. 2015.
[3] X.-Y. Lin, T.-W. Ho, C.-C. Fang, Z.-S. Yen, B.-J. Yang, and F. Lai, "A mobile indoor positioning system based on iBeacon technology," in *Proc. IEEE EMBC*, Milan, Italy, Aug. 2015, pp. 4970–4973.
[4] C.-H. Huang, L.-H. Lee, C. C. Ho, L.-L. Wu, and Z.-H. Lai, "Real-time RFID indoor positioning system based on Kalman-filter drift removal and Heron-bilateration location estimation," *IEEE Trans. Instrum. Meas.*, vol. 64, no. 3, pp. 728–739, Mar. 2015.
[5] R. Harle, "A survey of indoor inertial positioning systems for pedestrians," *IEEE Commun. Surveys Tuts.*, vol. 15, no. 3, pp. 1281–1293, Jul. 2013.
[6] X. Du, K. Yang, and D. Zhou, "Mapsense: Mitigating inconsistent WiFi signals using signal patterns and pathway map for indoor positioning," *IEEE Internet Things J.*, to be published.
[7] C. Park and S. H. Rhee, "Indoor positioning using Wi-Fi fingerprint with signal clustering," in *Proc. IEEE ICTC*, Jeju, South Korea, Oct. 2017, pp. 820–822.
[8] X. Du and K. Yang, "A map-assisted WiFi AP placement algorithm enabling mobile device's indoor positioning," *IEEE Syst. J.*, vol. 11, no. 3, pp. 1467–1475, Sep. 2017.
[9] M. Zhang, W. Shen, Z. Yao, and J. Zhu, "Multiple information fusion indoor location algorithm based on WiFi and improved PDR," in *Proc. IEEE CCC*, Chengdu, China, Jul. 2016, pp. 5086–5092.
[10] H. Xujian and W. Hao, "WiFi indoor positioning algorithm based on improved Kalman filtering," in *Proc. IEEE ICITBS*, Changsha, China, Dec. 2016, pp. 349–352.
[11] H. Nurminen, M. Raitoharju, and R. Piché, "An efficient indoor positioning particle filter using a floor-plan based proposal distribution," in *Proc. IEEE FUSION*, Heidelberg, Germany, Jul. 2016, pp. 541–548.
[12] Y. Zhang, Y. Zhu, F. Yan, L. Shen, and T. Song, "Indoor positioning and tracking using particle filters with suboptimal importance density," in *Proc. IEEE VTC-Fall*, Montreal, QC, Canada, Sep. 2016, pp. 1–5.
[13] I. Masmitja, P. J. Bouvet, S. Gomariz, J. Aguzzi, and J. del Rio, "Underwater mobile target tracking with particle filter using an autonomous vehicle," in *Proc. IEEE ENC*, Helsinki, Finland, Jun. 2016, pp. 1–9.

[14] N. Hassan, S. Mathavan, and K. Kamal, "Road crack detection using the particle filter," in *Proc. IEEE ICAC*, Huddersfield, U.K., Sep. 2017, pp. 1–6.
[15] L. Yao, Y.-W. A. Wu, L. Yao, and Z. Z. Liao, "An integrated IMU and UWB sensor based indoor positioning system," in *Proc. IEEE IPIN*, Sapporo, Japan, Sep. 2017, pp. 1–8.
[16] W. Xue, W. Qiu, X. Hua, and K. Yu, "Improved Wi-Fi RSSI measurement for indoor localization," *IEEE Sensors J.*, vol. 17, no. 7, pp. 2224–2230, Apr. 2017.
[17] T. Parthornratt and K. Techakittiroj, "Improving accuracy of WiFi positioning system by using geographical information system (GIS)," in *Proc. IEEE Wireless Telecommun. Symp.*, Pomana, CA, USA, Apr. 2006, pp. 1–6.
[18] P. Bahl and V. N. Padmanabhan, "RADAR: An in-building RF-based user location and tracking system," in *Proc. IEEE INFOCOM*, Tel Aviv, Israel, vol. 2, Mar. 2000, pp. 775–784.
[19] H. X. Jian and W. Hao, "WiFi indoor location optimization method based on position fingerprint algorithm," in *Proc. IEEE ICSGEA*, Changsha, China, May 2017, pp. 585–588.
[20] J. Lategahn, M. Müller, and C. Röhrig, "Robust pedestrian localization in indoor environments with an IMU aided TDoA system," in *Proc. IPIN*, Busan, South Korea, 2014, pp. 465–472.
[21] C. Huang, S. He, Z. Jiang, C. Li, Y. Wang, and X. Wang, "Indoor positioning system based on improved PDR and magnetic calibration using smartphone," in *Proc. PIMRC*, Washington, DC, USA, 2014, pp. 2099–2103.
[22] Z. Yang, X. Feng, and Q. Zhang, "Adometer: Push the limit of pedestrian indoor localization through cooperation," *IEEE Trans. Mobile Comput.*, vol. 13, no. 11, pp. 2473–2483, Nov. 2014.
[23] A. Springer, W. Gugler, M. Huemer, L. Reindl, C. C. W. Ruppel, and R. Weigel, "Spread spectrum communications using chirp signals," in *Proc. IEEE EUROCOMM*, Munich, Germany, May 2000, pp. 166–170.
[24] C. Wang, Z. Zhang, L. Wu, and J. Dang, "High-precision multiple-antenna indoor positioning system based on chirp signal," in *Proc. IEEE WCSP*, Nanjing, China, Oct. 2017, pp. 1–5.
[25] P. Zietek, J. Kolakowski, and J. Modelski, "Improved method for TDOA estimation with chirp signals," in *Proc. IEEE Eur. Microw. Conf.*, Manchester, U.K., Oct. 2011, pp. 83–86.
[26] H. Farrokhi, "TOA estimation using MUSIC super-resolution techniques for an indoor audible chirp ranging system," in *Proc. IEEE Int. Conf. Signal Process. Commun.*, Dubai, United Arab Emirates, Nov. 2007, pp. 987–990.
[27] X. Ge, J. Yang, H. Gharavi, and Y. Sun, "Energy efficiency challenges of 5G small cell networks," *IEEE Commun. Mag.*, vol. 55, no. 5, pp. 184–191, May 2017.
[28] B. Gui and Q. Shen, "Research on emotional word clustering based on affinity propagation," in *Proc. IEEE CIS*, Hong Kong, Dec. 2017, pp. 151–154.
[29] C. Liu, R. Hey, and W. Wang, "K-AP clustering algorithm for large scale dataset," in *Proc. IEEE Int. Workshop Complex. Data Mining*, Nanjing, Jiangsu, Sep. 2011, pp. 87–89.
[30] A. G. Ponce, J. R. Marcial-Romero, J. A. Henrández, and G. De Ita, "An algorithm to approximate the chromatic number of graphs," in *Proc. IEEE CONIELECOMP*, Cholula, Puebla, Feb. 2015, pp. 110–115.
[31] N. J. Gordon, D. J. Salmond, and A. F. M. Smith, "Novel approach to nonlinear/non-Gaussian Bayesian state estimation," *IEE Proc. F-Radar Signal Process.*, vol. 140, no. 2, pp. 107–113, Apr. 1993.

XIAOFENG LU received the B.Sc. degree from Sichuan University, Chengdu, China, in 1996, the M.Sc. degree from Hunan University, Changsha, China, in 1999, and the Ph.D. degree in communication and information systems from the Huazhong University of Science and Technology, Wuhan, China, in 2006. From 1999 to 2003, he was a Research and Development Engineer with the Wuhan Research Institute of Post and Telecommunications. He is currently an Associate Professor with the State Key Laboratory of Integrated Services Networks, Xidian University, Xi'an, China. His main research interests lie in the area of broadband wireless communications, including resource allocation and virtualization, MU-MIMO, and OFDMA.

KUN YANG received the the M.Sc. and B.Sc. degrees from the Computer Science Department, Jilin University, China, and Ph.D. degree from the Department of Electronic and Electrical Engineering, University College London (UCL), U.K. He is currently a Full Professor with the School of Computer Science and Electronic Engineering, University of Essex, U.K. Before joining the University of Essex, in 2003, he was with UCL on several European Union research projects for several years. His main research interests include heterogeneous wireless networks, fixed mobile convergence, future Internet technology and network virtualization, cloud computing. He has published over 60 journal papers. He is a Senior Member of the IEEE and a Fellow of IET. He serves on the editorial boards of both the IEEE and non-IEEE journals.

JIAYU LIU was born in Shaanxi, China. She received the B.Sc. degree in communication engineering from Xidian University, Xi'an, China, in 2014, where she is currently pursuing the M.Sc. degree in communication and information system with the State Key Laboratory of Integrated Service Networks. Her research interests include indoor localization, machine learning, and collaborative filtering system for LBS.

CHANGLIN YANG was born in Henan, China. He received the B.Sc. degree in electronic information engineering from Zhengzhou University, Zhengzhou, China, in 2016. He is currently pursuing the M.Sc. degree in electronic and communication engineering with the State Key Laboratory of Integrated Service Networks, Xidian University, Xi'an. His research interests include Indoor localization, software-defined wireless network, and LBS.

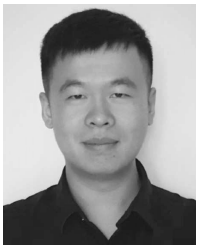

ZIBO ZHANG was born in Anhui, China. He received the B.Sc. degree in electronic information engineering from Xidian University, Xi'an, China, in 2015, and the M.Sc. degree in electronic and communication engineering from the State Key Laboratory of Integrated Service Networks, Xidian University. His research interests include indoor localization, android application development, software-defined wireless network, and LBS.

HAILIN ZHANG received the B.S. and M.S. degrees from Northwestern Polytechnic University, Xi'an, China, in 1985 and 1988, respectively, and the Ph.D. degree from Xidian University, Xi'an, in 1991, where he is currently a Full Professor and the Head of the School of Telecommunications Engineering. His main research interests include the area of broadband wireless communications, including massive MIMO, OFDM, and space-time coding. He has recently published 78 papers in telecommunications journals and proceedings.